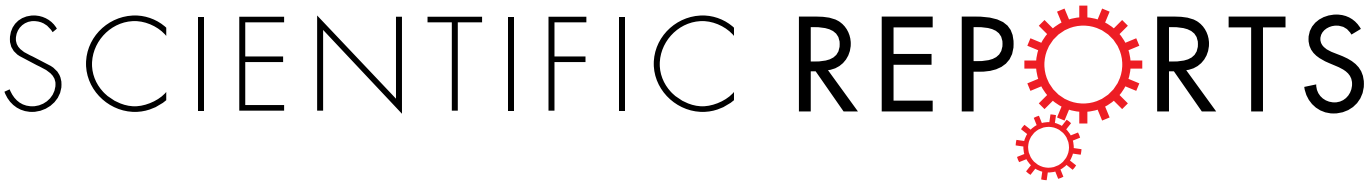

OPEN

Isotopic evidence for temperate oceans during the Cambrian Explosion

Received: 1 May 2018
Accepted: 2 April 2019
Published online: 19 April 2019

Thomas Wotte[1], Christian B. Skovsted[2], Martin J. Whitehouse[3] & Artem Kouchinsky[2]

The Cambrian Explosion was a key event in the evolution of life on Earth. This event took place at a time when sea surface temperatures have been proposed to reach about 60 °C. Such high temperatures are clearly above the upper thermal limit of 38 °C for modern marine invertebrates and preclude a major biological revolution. To address this dichotomy, we performed *in situ* $\delta^{18}O$ analyses of Cambrian phosphatic brachiopods via secondary ion mass spectrometry (SIMS). The $\delta^{18}O_{phosphate}$ data, which are considered to represent the most primary $\delta^{18}O_{seawater}$ signature, were identified by evaluating the diagenetic alteration of the analyzed shells. Assuming ice-free conditions for the Cambrian ocean and no change in $\delta^{18}O_{seawater}$ (-1.4‰ to -1‰; V-SMOW) through time, our temperatures vary between 35 °C ± 12 °C and 41 °C ± 12 °C. They are thus clearly above (1) recent subequatorial sea surface temperatures of 27 °C–35 °C and (2) the upper lethal limit of 38 °C of marine organisms. Our new data can therefore be used to infer a minimal depletion in early Cambrian $\delta^{18}O_{seawater}$ relative to today of about -3‰. With this presumption, our most pristine $\delta^{18}O_{phosphate}$ values translate into sea surface temperatures of about 30 °C indicating habitable temperatures for subequatorial oceans during the Cambrian Explosion.

The Cambrian Explosion was one of the most important events in the history of life on Earth. Within a few million years, the simple life of the Precambrian evolved to highly organized organisms with modern anatomical characteristics such as a chorda dorsalis, complex eyes and legs, and biomineralized skeletal parts[1–5]. During this fundamental biotic event, the metazoans invaded all kinds of marine habitats and evolved complex ecosystems and food webs for the first time[6,7]. Insights into this often odd-looking Cambrian world are provided by a variety of global fossil Lagerstätten such as the Burgess Shale (Canada)[8], Chengjiang (South China)[9], or Sirius Passet (Greenland)[10] (Fig. 1). The reasons for this radical faunal turnover are still poorly understood but changes in ocean chemistry[11,12], the rise in atmospheric and oceanic oxygen concentration to modern levels[13,14], and the presumed evolutionary arms race between predators and prey[15,16] have been discussed as major driving mechanisms. Additionally, the establishment of habitable seawater temperatures seems to be most essential for the evolution of diverse marine metazoan life. Information on marine paleotemperatures is inferred from studies of oxygen isotopes ($\delta^{18}O$) from bulk carbonate samples, marine cements, cherts, phosphorites, or fossils of calcitic or phosphatic composition. However, independent of the material analyzed, these oxygen isotope ratios become progressively depleted in the heavier ^{18}O towards older stratigraphic units[17–20], resulting in a rising trend of reconstructed seawater temperatures with increasing age. For the Cambrian, temperatures of about 60 °C or even higher have been proposed[17–23], which is intolerable for most animals in modern oceans. Whether this trend reflects (1) an increased diagenetic alteration of older rocks, (2) secular changes in the oxygen isotopic composition of ancient ocean seawater, or (3) higher original seawater temperatures in the past, is still controversial[17–23]. If seawater oxygen isotope composition is considered as constant throughout Earth history, a $\delta^{18}O$ value of ~ -1‰ is generally assumed to characterize an ice-free planet[24]. In contrast, assuming that seawater $\delta^{18}O$ changed substantially over time, a global average of Cambrian seawater $\delta^{18}O$ of up to -6.5‰ or even -8‰ has been proposed[25]. These presumptions would shift the reconstructed temperature of ancient seawater towards higher or lower values, respectively.

[1]Institut für Geologie, TU Bergakademie Freiberg, Bernhard-von-Cotta-Straße 2, D-09599, Freiberg, Germany. [2]Department of Palaeobiology, Swedish Museum of Natural History, Box 50007, SE-104 05, Stockholm, Sweden. [3]Department of Geosciences, Swedish Museum of Natural History, Box 50007, SE-104 05, Stockholm, Sweden. Correspondence and requests for materials should be addressed to T.W. (email: thomas.wotte@geo.tu-freiberg.de)

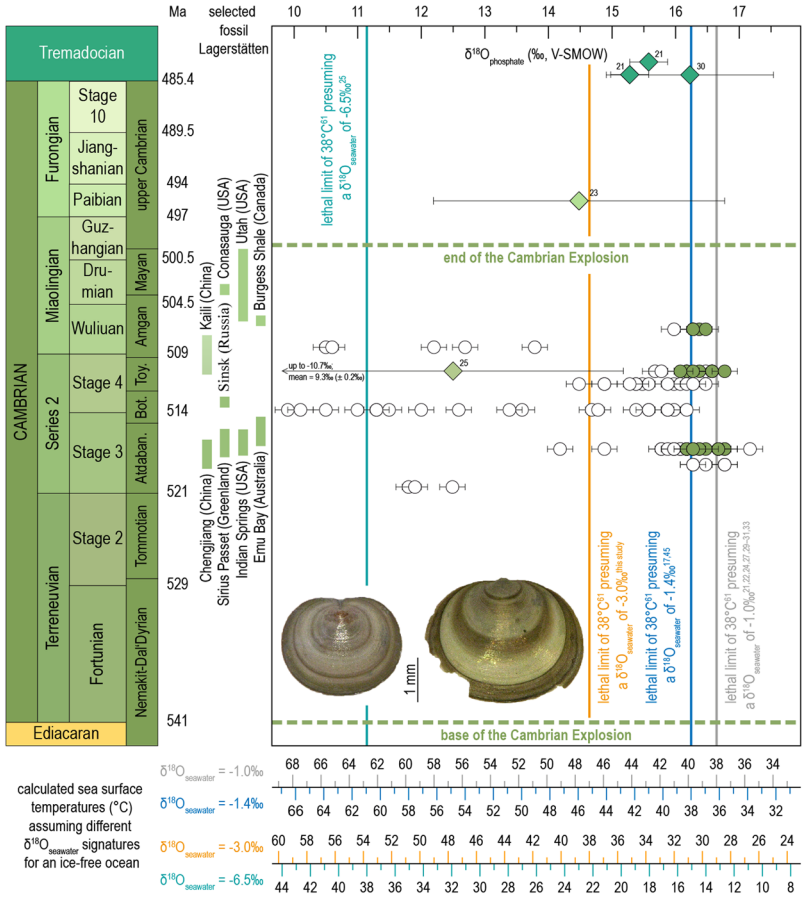

Figure 1. Oxygen isotope compositions of Cambrian and Tremadocian brachiopods and conodonts. Our $\delta^{18}O_{phosphate}$ data range from 9.9‰ to 17.2‰ (V-SMOW; 1σ ± 0.2‰). Calculated seawater surface temperatures assuming $\delta^{18}O_{seawater}$ signatures of -1.0‰[21,22,24,27,29–31,33] and -1.4‰[17,45] vary between 34 °C ± 12 °C and 68 °C ± 11 °C. Excluding altered and probably altered $\delta^{18}O_{phosphate}$ data, our calculated sea surface temperatures range from 35 °C ± 12 °C to 41 °C ± 12 °C. In contrast, assuming a Cambrian $\delta^{18}O_{seawater}$ signature of -6.5‰[25], reconstructed sea surface temperatures are incredible low, ranging from 12 °C ± 14 °C to 16 °C ± 14 °C. Our new data therefore clearly support the hypothesis of a secular change in the ocean $\delta^{18}O$ during Earth history. A minimal depletion in early Cambrian $\delta^{18}O_{seawater}$ relative to today of about -3‰ is assumed. With this presumption, our most pristine $\delta^{18}O_{phosphate}$ values translate into sea surface temperatures of 28 °C ± 13 °C to 32 °C ± 13 °C. Our most pristine $\delta^{18}O_{phosphate}$ values are illustrated by green circles, (probably) altered data by white circles. Additional data points of the Cambrian Series 2–Tremadocian were generated from bulk sample analyses of conodonts and brachiopods[23,30] and *in situ* measurements of conodonts[21] and brachiopods[25]. SIMS data of ref.[25] vary between -10.6‰ (±0.1‰) and 14.8‰ (±0.4‰); mean = 9.3‰ (±0.2‰). Global Cambrian time scale and selected fossil Lagerstätten are from ref.[38,43]. Siberian nomenclature from ref.[41]. Atdaban. = Atdabanian Stage, Bot. = Botoman Stage, Toy. = Toyonian Stage.

Oxygen isotopes of marine carbonates ($\delta^{18}O_{carbonate}$) have been used for studies of seawater temperatures since the beginning of geochemical research. One drawback of carbonate mineralogy is its susceptibility to diagenetic alteration, making the application of $\delta^{18}O_{carbonate}$ more doubtful for older stratigraphic successions which are typically characterized by intense alteration and recrystallization. The analysis of phosphate minerals (i.e. apatite), which are considered to be more resistant to diagenetic processes than carbonate, are therefore an attractive alternative, or at least a complementary tool, for assessing paleoclimate conditions[18,26,27]. In Paleozoic successions, conodonts and phosphatic brachiopods have been used in addition to calcite-shelled brachiopods to provide information about the seawater temperatures via their oxygen isotope composition with high stratigraphic resolution[27–29]. Seawater temperatures calculated from $\delta^{18}O_{phosphate}$ vary between 36 and 53 °C (or even 62 °C) for the late Cambrian (brachiopods)[23] and between 33 and 41 °C for the Early Ordovician (Tremadocian; brachiopods and conodonts)[30], in both cases assuming an ice-free ocean and no significant change in $\delta^{18}O_{seawater}$ over time. However, the traditional $\delta^{18}O$ method of analysis of phosphates requires bulk samples of about 0.5–1 mg[29,31] which equates to several hundred conodont elements or several complete brachiopod shells depending on their size and weight. The pooling of various specimens may result in significant problems. Even if carefully evaluated, sampling of altered material cannot be avoided with certainty as these areas are not observable macroscopically. Incorporation of only a fraction of altered sample material will result in $\delta^{18}O_{phosphate}$ data that do not represent the

primary oxygen isotopic composition of ambient seawater. A possible alternative may be the analysis of clumped isotopes, which could allow the discrimination of the diagenetic isotopic signal from the primary one[32]. A critical drawback of this method, however, is the enormous sample size of up to 12 mg and 200 mg required for calcite and phosphate samples, respectively[32]. Against this background, *in situ* measurements of oxygen isotopes have been applied using SIMS and similar high precision *in situ* analyses[21,25,33–37], which minimize sample sizes and therefore the risk of contamination of the primary oxygen isotope signal. Again, assuming ice-free conditions and no significant variation in seawater $\delta^{18}O$ over time, the corresponding values of Ordovician $\delta^{18}O_{conodont}$ in such analyses range from 15.3‰ to 19.6‰ (V-SMOW)[21]. Temperatures calculated from these values vary from 25 °C to 44 °C[21]. Even higher calculated temperatures are reported from middle Cambrian brachiopods with a mean value of 71 °C ± 11 °C and a minimum temperature of 46 °C ± 10 °C[25]. However, assuming a Cambrian $\delta^{18}O$ seawater composition of -6.5‰ these Cambrian temperatures were re-calculated to a minimum seawater temperature of 22 °C ± 10 °C (mean value of 47 °C ± 12 °C) and interpreted to represent the original seawater temperature of early–middle Cambrian southern latitudes (65°S to 70°S)[25].

Here we present a study of *in situ* oxygen isotope analyses of Cambrian phosphatic brachiopods using the SIMS technique (CAMECA ims1280 at the Nordsim laboratory, Swedish Museum of Natural History, Stockholm), in order to shed new light on the unexpected high seawater temperatures estimated for the Cambrian Period and their aforementioned implications.

Stratigraphic Setting and Material

Thirteen exceptionally conserved Cambrian lingulid and acrotetid brachiopod shells (Fig. 1; Supplementary Material) were analyzed for their oxygen isotopic composition. The shells are composed of fluorapatite. They come from the Siberian Platform which is characterized by an almost horizontally bedded Cambrian sedimentary succession showing no or only minor metamorphic or tectonic overprint. Within the sedimentary rocks covering the Terreneuvian–Miaolingian[38] interval, three distinct facies realms are developed, characterizing an eastward deepening of the depositional environment[39,40]. From west to east these are the restricted–lagoonal Turukhansk-Irkutsk-Olekma, the open marine Yudoma-Olenek, and the transitional Anabar-Sinsk facies realms (Fig. 2). The thirteen brachiopods analyzed herein belong to the open marine Yudoma-Olenek facies realm. Sections investigated are located along the Malaya Kuonamka (sections 96-1 and 96B-1) and Bol'shaya Kuonamka (sections 96-7, 96B-7, and 96-8) rivers on the eastern flank of the Anabar Uplift of the Siberian Platform (Fig. 2). The fauna from the sections includes trilobites, brachiopods, echinoderms, and other shelly fossils[41] typical for shallow marine Cambrian carbonate environments with normal salinity.

Samples cover the Tommotian–Amgan interval (according to the Siberian nomenclature[41,42]) respectively the Terreneuvian (Cambrian Stage 2)–Miaolingian (Wuliuan Stage) interval (according to the international nomenclature[38,43]; Figs 1 and 2), and thus offer a unique window into the time of the Cambrian Explosion.

Results

Calculation of seawater temperatures. Ninety-six spots on 13 brachiopod shells were analyzed for their oxygen isotopic composition. The $\delta^{18}O_{phosphate}$ values obtained range from 9.9‰ to 17.2‰ (V-SMOW; 1σ ± 0.2‰). Oxygen isotope data vary between specimens, but also show intra-sample variations of about 3‰ up to 6‰ (samples 1599-16, 1599-38, 1599-39; see Supplementary Table 1). For calculation of paleotemperature we applied the equation of Lécuyer and co-authors[44]. The major part of the Terreneuvian–Miaolingian interval is considered as an ice-free period. Assuming (1) an ice-free Cambrian ocean and therefore a $\delta^{18}O_{seawater}$ value of -1.0‰[21,22,24,27,29–31,33] or -1.4‰[17,45], and (2) considering error propagation, our reconstructed sea surface temperatures vary between 34 °C ± 12 °C and 68 °C ± 11 °C, (Fig. 1, and see Supplementary Material for additional information). In contrast, presuming an increasing $\delta^{18}O_{seawater}$ over time and a global Cambrian ocean average $\delta^{18}O$ of -6.5‰[25], calculated temperatures become incredible cooler, ranging from 11 °C ± 14 °C to 44 °C ± 12 °C (Fig. 1).

Diagenetic constraints. It is generally considered, that phosphate minerals are less susceptible to diagenetic alteration than carbonates. However, several studies indicate that skeletal phosphate minerals are metastable and were typically recrystallized during early diagenesis[17,46,47]. Whereas no widespread diagenetic processes are known to result in an enrichment of ^{18}O in phosphates[17], more negative $\delta^{18}O$ values are generally considered as a sign of diagenetic alteration[27].

In our samples, reflected light optical images already indicate recrystallization of individual shells and shell portions, which are characterized by considerably darker color and inhomogeneous appearance (Supplementary Material). SEM photographs confirm this first order identification by revealing the brachiopod shell ultrastructure in detail (Fig. 3; Supplementary Material). Dense crystalline shell material without any indication for recrystallization and alteration is characterized by $\delta^{18}O_{phosphate}$ values generally more positive than 16.0‰, which thus appear to represent the most primary $\delta^{18}O_{seawater}$ signature. Pores, laminae, and secondary fissures in other shell portions potentially act as pathways for fluid migration and therewith for diagenetic alteration. The visually identified recrystallized shells or portions of shells often, if not ubiquitously, yield lower $\delta^{18}O_{phosphate}$ values, and are thus interpreted as most probably diagenetically altered (see Fig. 1 and Supplementary Material). Even for spots showing only initial recrystallization or partially pores, diagenetic alteration cannot be excluded with certainty. All these (probably) altered data are not included in our final discussion. The co-occurrence of both, dense crystalline and recrystallized areas in one and the same shell also explains large intra-shell variations as identified in samples 1599-16, 1599-38, or 1599-39.

Analytical constrains. Despite the obvious advantages of $\delta^{18}O$ analyses on biogenic apatite using SIMS (e.g., analyses of very small samples or distinct shell portions), a number of sources for probable errors have to be addressed, not all of which are presently fully understood. The general chemical formula of apatite $Ca_5(PO_4$,

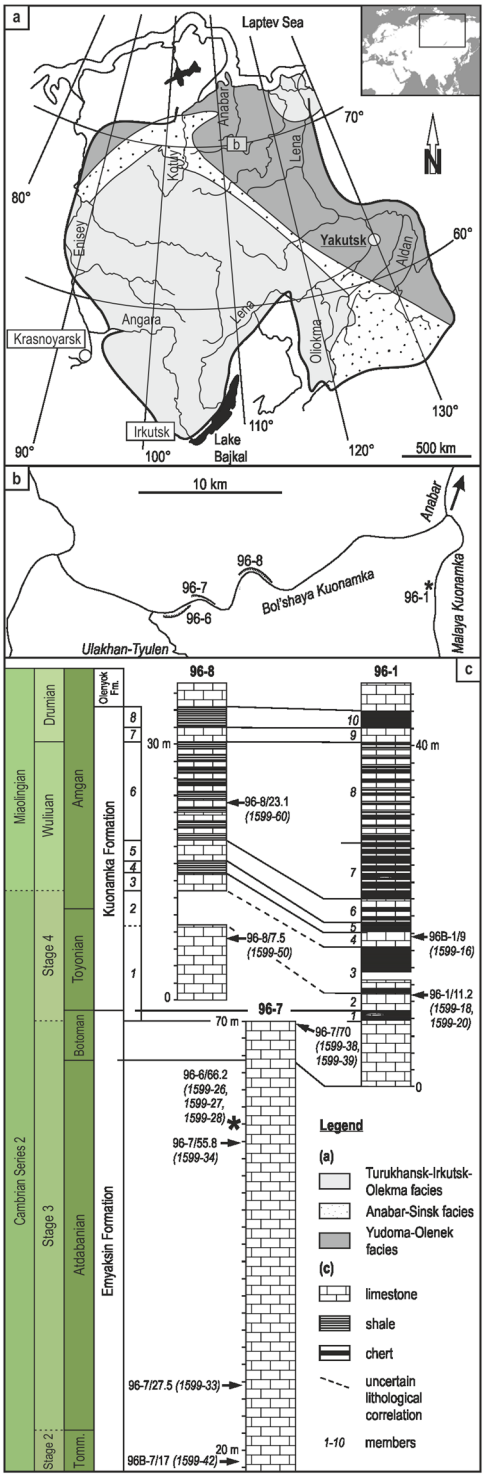

Figure 2. Geology of the sample area and stratigraphy of the samples. (**a**) Geological map of the northern Siberian Platform. (**b**) Geographic positions of the sections investigated. Section 96-1 is located on the Malaya Kuonamka River, sections 96-6, 96-7, and 96-8 are located on the Bol'shaya Kuonamka River. (**c**) Stratigraphic columns of the sections investigated. Derivation of brachiopod samples analyzed herein are marked by arrows with numbers. Tomm. = Tommotian Stage, Fm. = Formation.

$CO_3)_3(CO_3, F, OH)$ contains three common oxygen bearing molecular groups. Whereas $\delta^{18}O_{phosphate}$ analyses performed by the conventional IRMS method only isolate the PO_4^{3-} group as trisilverphosphate (Ag_3PO_4) and subsequently analyze the oxygen isotopes by high-temperature reduction[27,29,31,37,48], the SIMS technique indiscriminately samples oxygen from PO_4^{3-}, CO_3^{2-}, OH^-, as well as residual organics[36,49]. The integration of oxygen

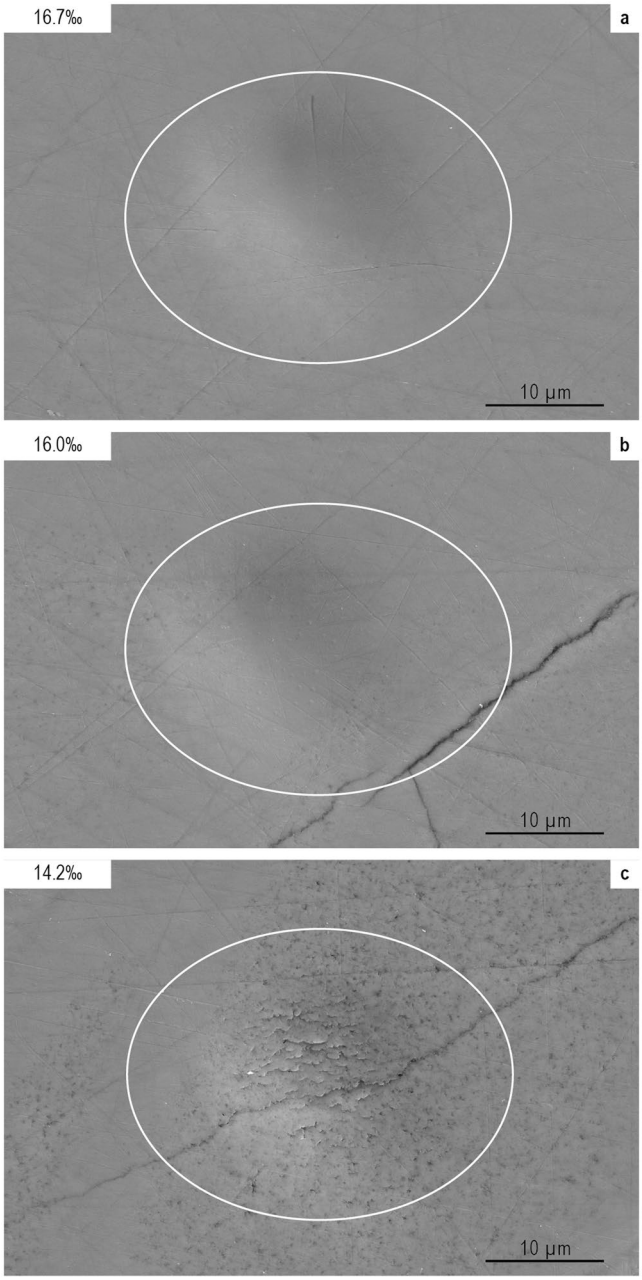

Figure 3. SEM images of selected spots from sample 1599-28 showing different stages of alteration. (**a**) Dense material (e.g., spot 1; 16.7‰) without any indication for recrystallization processes is generally characterized by more positive $\delta^{18}O_{phosphate}$ values. We interpret such parts as representing the most primary $\delta^{18}O_{seawater}$ signature. (**b**) Slightly more negative $\delta^{18}O_{phosphate}$ values (e.g., spot 3; 16.0‰) most probably mirror diagenetic alteration caused by pores, fractures, or laminae acting as pathways for fluid migration. (**c**) Fractures and recrystallized shell material correspond to a considerably lower $\delta^{18}O_{phosphate}$ values (spot 6; 14.2%), thus appear to represent diagenetically altered shell portions.

from these different sources will likely influence the SIMS-determined $\delta^{18}O_{phosphate}$ values. This problem is relevant when analyzing e.g. organo-phosphatic brachiopods characterized by an alternation of carbonate-fluorapatite and organic-rich laminae. Studies on recent and fossil lingulid brachiopods have documented intra-shell $\delta^{18}O_{phosphate}$ variations often exceeding 4‰ that probably represent vital fractionation effects[50]. Similar intra-element $\delta^{18}O_{phosphate}$ variations were detected from conodonts[36]. Therefore, care should be taken when interpreting $\delta^{18}O_{phosphate}$ values generated by SIMS. However, variations in $\delta^{18}O_{phosphate}$ can be minimized by high spatial resolution SIMS analyses on the most pristine areas[36].

Multitude of paired SIMS and IRMS $\delta^{18}O_{phosphate}$ analyses on conodonts have shown, that SIMS normally yields values 0.5–1.0‰ higher[21,33,35,36]. There is still uncertainty about the systematic offset between both methods in measuring the $\delta^{18}O_{phosphate}$ values in phosphate brachiopods. This unknown offset would of course bias the

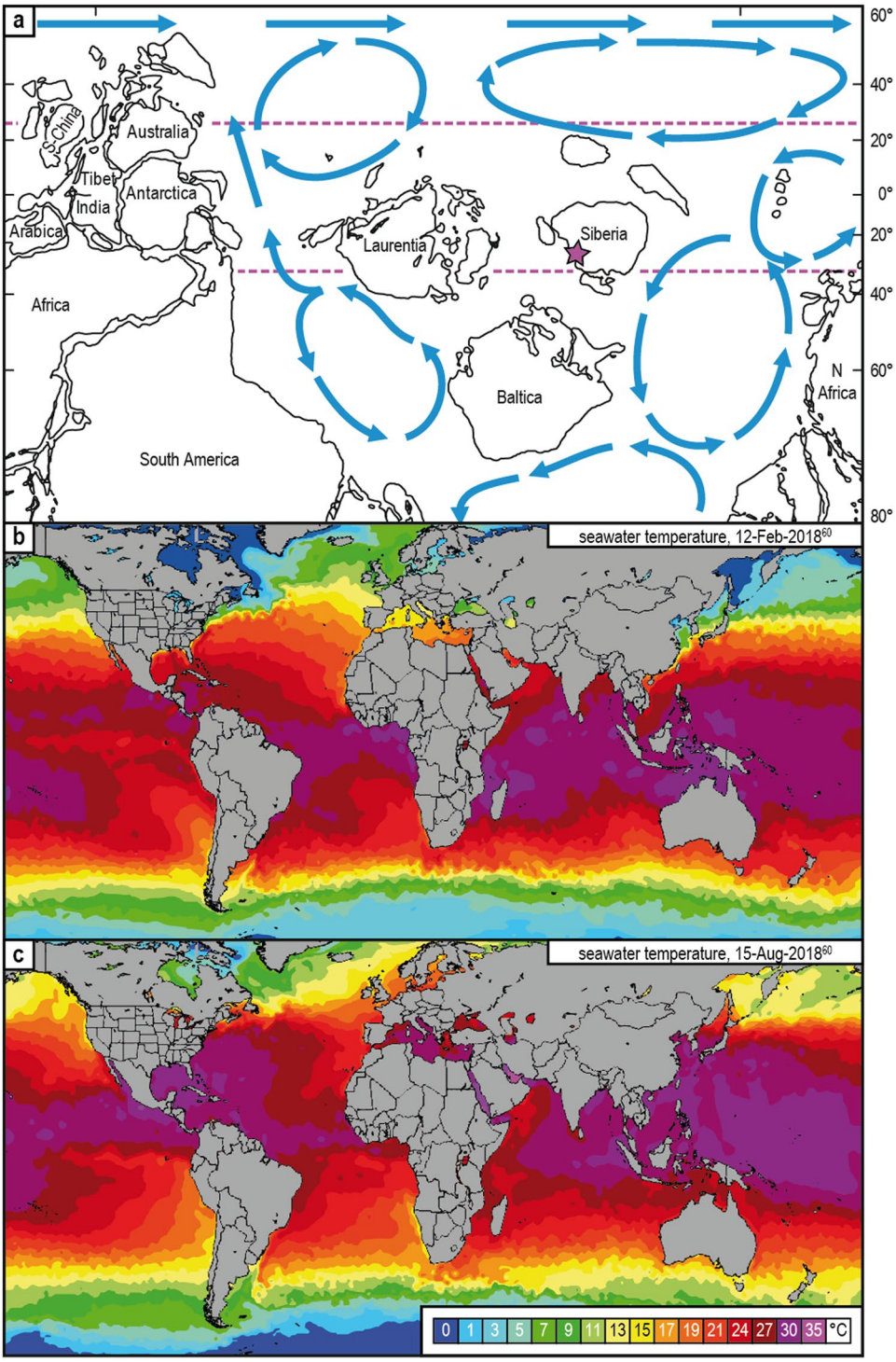

Figure 4. Reconstruction of the Terreneuvian earth and illustration of the recent seawater temperature. (**a**) Reconstruction of lower Cambrian paleogeography and ocean currents (blue arrows). Dotted purple lines correspond with the 35 °C isotherms of ref.[25]. The location of the sections investigated has been identified (purple star). (**b,c**) Illustration of the current seawater temperatures during austral summer (**b**)/winter (**c**) is based on the open source ref.[60]. Recent subequatorial seawater temperatures vary between 24 °C and 27 °C (austral winter) and between 27 °C and 35 °C (austral summer). Comparable mean annual temperatures could be also assumed for the Siberian carbonate shelf, located in a similar paleogeographic position during the Terreneuvian–Cambrian Series 2 interval.

calculation of paleotemperatures to higher values. In this context it should be also mentioned, that coefficients in the available thermometer equations[44,51,52] were determined by IRMS (isotope ratio mass spectrometer) analyses. Whether these equations have to be adjusted for treatment of SIMS data, needs further investigation.

A probable further weakness arises from the Durango apatite standard which is commonly used to calibrate the $\delta^{18}O_{phosphate}$ measurements generated by SIMS. Crystals of Durango apatite are generally assumed to be homogeneous in $\delta^{18}O$[53,54]. A recent study, however, questions this presumption and identifies conspicuous intra-crystalline heterogeneity in $\delta^{18}O$ in all apatite standards available[53]. However, $\delta^{18}O$ analyses of our samples and in house Durango apatite were performed on restricted crystal portions and $\delta^{18}O_{Durango}$ values show no significant variation and a reproducibility generally better than ±0.2‰ (1σ).

Discussion

Biological and paleogeographical considerations. During the early and middle Cambrian, Siberia was located in a subtropical position south of the equator[55] (Fig. 4a). Most recent simulations indicate mean sea surface temperatures of more than 35 °C for this paleogeographic region with minimum and maximum values of about 33 °C (austral winter) and 40 °C (austral summer), respectively[25]. Similar data were modeled for Furongian to the middle Silurian equatorial to subequatorial oceans, with values varying between 30 and 35 °C[56]. Comparable warm temperate ocean conditions of about 30 °C with maxima up to 37 °C (or even approaching 40 °C) are not unusual in earth history. They have also been estimated for the Triassic, Middle Jurassic, and Cretaceous times[57–59].

Average temperatures of present subequatorial ocean areas of comparable latitude to the position of Siberia in the early Cambrian vary between 24 °C (austral winter) and 35 °C (austral summer), respectively[60] (e.g., eastern Indian ocean, Java-, Banda-, Timor-, and Arafura seas; Fig. 4b,c). Assuming an ice-free Cambrian ocean and a $\delta^{18}O_{seawater}$ value of -1.0‰[21,22,24,27,29–31,33] or -1.4‰[17,45], our temperatures calculated from the most primary $\delta^{18}O_{phosphate}$ values vary between 35 °C ± 12 °C and 41 °C ± 12 °C. They are thus clearly higher than modern annual subequatorial temperatures. They also often exceed the upper lethal temperature for modern marine species which is typically considered to be 38 °C with habitat-dependent fluctuations towards higher and lower values[61–64]. The biological tolerance limit of 38 °C can be probably applied to Cambrian life forms, even if modern restrictions may not be strictly assumed for deep geological time.

Implications for the interpretation of the Paleozoic seawater temperature. Considering the thermal limit of 38 °C as a critical threshold, secular changes in the oxygen isotopic composition of ocean seawater are necessary to explain the presence of marine life in the Paleozoic. Based on our interpretation of the Siberian data a minimal depletion in oxygen isotopic composition of early–middle Cambrian seawater relative to today would be about -3‰. With this assumption and excluding altered and probably altered $\delta^{18}O_{phosphate}$ values, calculated subtropical sea surface temperatures vary between 28 °C ± 13 °C and 32 °C ± 13 °C (Fig. 1). The minimum temperature becomes even lower (26 °C ± 13 °C) if we involve the most positive $\delta^{18}O_{phosphate}$ value (17.2‰) into our calculation. These sea surface temperatures would be (1) clearly below the upper lethal limit of 38 °C of marine organisms (Fig. 1) and (2) comparable to temperatures of present subequatorial ocean areas (Fig. 4). Unexpected high temperatures calculated from the *in situ* measurements and bulk sample analyses of brachiopods[23,25] for the Cambrian are thus most probably an artifact of diagenetic alteration. However, the possibility of larger ^{18}O depletions up to -6.5‰ or even -8‰[25] cannot be excluded completely if (1) the observed spread of data in our samples represent more than just an artifact of alteration and/or (2) other thermometer equations (e.g., Pucéat and co-authors[52]) are applied for temperature calculation.

Methods

Oxygen isotope analyses. For oxygen isotope ($\delta^{18}O$) analyses, brachiopod shells were mounted centrally on two-side tape fixed on a 4.5 × 4.5 cm acrylic glass (Supplementary Material). Six grains of an in house Durango apatite standard were added and both (samples and standard) were embedded in an epoxy pellet of 2.5 cm in diameter. After hardening of about 24 hours, pellets were removed from the tape and polished to a low relief in order to minimize analytical artifacts[65,66]. To facilitate navigation during SIMS analyses, a photograph image of the stub was generated using the Olympus cellSens Standard software (Supplementary Material). Prior to measurements, samples were coated with 30 nm of gold.

$\delta^{18}O$ analyses were performed on a CAMECA ims1280 large-geometry ion microprobe at the Department of Geosciences of the Swedish Museum of Natural History (Nordsim facility). For analyses, a $^{133}Cs^{+}$ ion beam with an intensity of ~3 nA was critically focused and a small raster applied to homogenize the beam profile on the sample, resulting in an analyzed volume of about 10 µm width and about 2 µm depth. For calibration, two–four analyses of the Durango apatite were performed before and after six analyses of brachiopod shells. Results are reported in ‰ relative to the V-SMOW (Vienna Standard Mean Ocean Water) standard with reproducibility generally better than ± 0.2‰ (1σ). A total of 134 measurements (96 samples and 38 standard) was performed (Supplementary Material & Supplementary Table 1). Parallel to oxygen isotope measurements each analyzing spot and surrounding shell material was imaged.

Scanning electron microscopy and energy-dispersive X-ray spectroscopy. Scanning electron microscopy (SEM) was performed on the Zeiss Sigma 300 VP at the Department of Paleontology of the University of Cologne. We used the gold-coated stubs already utilized for $\delta^{18}O$ analyses. In addition to the SEM images, energy-dispersive X-ray spectroscopy (EDS or EDXS) was applied using a X-Max^{N} 80 Silicon Drift Detector (Oxford Instruments) connected to the SEM. No identification of inconsistencies in element concentration could be shown by the SEM-EDS analyses (see Supplementary Material for selected spots).

All data generated or analyzed during this study are included in this published article (and its Supplementary Material).

References

1. Shu, D.-G. *et al*. Lower Cambrian vertebrates from South China. *Nature* **402**, 42–46 (1999).
2. Lee, M. S. Y. *et al*. Modern optics in exceptionally preserved eyes of Early Cambrian arthropods from Australia. *Nature* **474**, 631–634 (2011).
3. Ma, X., Hou, X., Edgecombe, G. D. & Strausfeld, N. J. Complex brain and optic lobes in an early Cambrian arthropod. *Nature* **490**, 258–262 (2012).
4. Li, L., Zhang, X., Yun, H. & Li, G. Complex hierarchical microstructures of Cambrian mollusk *Pelagiella*: insight into early biomineralization and evolution. *Sci. Rep* **7**, 1935 (2017).
5. Zhao, F., Bottjer, D. J., Hu, S., Yin, Z. & Zhu, M. Complexity and diversity of eyes in Early Cambrian ecosystems. *Sci. Rep* **3**, 2751 (2013).
6. Conway-Morris, S. The Cambrian "explosion": Slow-fuse or megatonnage? *PNAS* **97**, 4426–4429 (2000).
7. Conway-Morris, S. The Cambrian "explosion" of metazoans and molecular biology: Would Darwin be satisfied? *Int. J. Dev. Biol.* **47**, 505–515 (2003).
8. Briggs, D. E. G., Erwin, D. H. & Collier, F. J. *The Fossils of the Burgess Shale*. Smithsonian Institution Press, 238 pp. (1994).
9. Hou, X.-G., Aldridge, R. J., Bergström, J., Siveter, D. J. & Feng, X.-H. *The Cambrian Fossils of Chengjang, China: The Flowering of Early Animal Life*. Blackwell Science Ltd., 233 pp. (2004).
10. Peel, J. S. & Ineson, J. R. The extent of the Sirius Passet Lagerstätte (early Cambrian) of North Greenland. *Bull. Geosci.* **86**, 535–543 (2011).
11. Brennan, S. T., Lowenstein, T. K. & Horita, J. Seawater chemistry and the advent of biocalcification. *Geology* **32**, 473–476 (2004).
12. Tatzel, M., von Blanckenburg, F., Oelze, M., Bouchez, J. & Hippler, D. Late Neoproterozoic seawater oxygenation by siliceous sponges. *Nat. Commun.* **8**, 621 (2017).
13. Shen, Y., Zhang, T. & Hoffman, P. F. On the coevolution of Ediacaran oceans and animals. *Proc. Natl. Acad. Sci. U.S.A.* **105**, 7376–7381 (2008).
14. Chen, X. *et al*. Rise to modern levels of ocean oxygenation coincided with the Cambrian radiation of animals. *Nat. Commun*. **6**, 7142 (2015).
15. Dzik, J. Behavioral and anatomical unity of the earliest burrowing animals and the cause of the "Cambrian explosion". *Paleobiol* **31**, 503–521 (2005).
16. Zhang, H. *et al*. Armored kinorhynch-like scalidophoran animals from the early Cambrian. *Sci. Rep* **5**, 16521 (2015).
17. Jaffrés, J. B. D., Shields, G. A. & Wallmann, K. The oxygen isotope evolution of seawater: A critical review of a long-standing controversy and an improved geological water cycle model for the past 3.4 billion years. *Earth-Sci. Rev.* **83**, 83–112 (2007).
18. Prokoph, A., Shields, G. A. & Veizer, J. Compilation and time-series analysis of a marine carbonate $\delta^{18}O$, $\delta^{13}C$, $^{87}Sr/^{86}Sr$ and $\delta^{34}S$ database through Earth history. *Earth-Sci. Rev.* **87**, 113–133 (2008).
19. Veizer, J. & Prokoph, A. Temperatures and oxygen isotopic composition of Phanerozoic oceans. *Earth-Sci. Rev.* **146**, 92–104 (2015).
20. Veizer, J. *et al*. $^{87}Sr/^{86}Sr$, $\delta^{13}C$ and $\delta^{18}O$ evolution of Phanerozoic seawater. *Chem. Geol.* **161**, 59–88 (1999).
21. Trotter, J. A., Williams, I. S., Barnes, C. R., Lécuyer, C. & Nicoll, R. S. Did cooling oceans trigger Ordovician biodiversification? Evidence from conodont thermometry. *Science* **321**, 550–554 (2008).
22. Wenzel, B. & Joachimski, M. M. Carbon and oxygen isotopic composition of Silurian brachiopods (Gotland/Sweden): palaeoceanographic implications. *Palaeogeogr. Palaeoclimatol. Palaeoecol* **122**, 143–166 (1996).
23. Elrick, M., Rieboldt, S., Saltzman, M. & McKay, R. M. Oxygen-isotope trends and seawater temperature changes across the Late Cambrian Steptoean positive carbon-isotope excursion (SPICE event). *Geology* **39**, 987–990 (2011).
24. Savin, S. M. The history of the earth's surface temperature during the past 100 million years. *Ann. Rev. Earth Planet. Sci* **5**, 319–355 (1977).
25. Hearing, T. W. *et al*. An early Cambrian greenhouse climate. *Sci. Adv.* **4**, eaar5690 (2018).
26. Mine, A. H. *et al*. Microprecipitation and $\delta^{18}O$ analysis of phosphate for paleoclimate and biogeochemistry research. *Chem. Geol.* **460**, 1–14 (2017).
27. Wenzel, B., Lécuyer, C. & Joachimski, M. M. Comparing oxygen isotope records of Silurian calcite and phosphate—$\delta^{18}O$ compositions of brachiopods and conodonts. *Geochim. Cosmochim. Acta* **64**, 1859–1872 (2000).
28. Luz, B., Kolodny, Y. & Novach, J. Oxygen isotope variations in phosphate of biogenic apatites, III. Conodonts. *Earth Planet. Sci. Lett.* **69**, 255–262 (1984).
29. Joachimski, M. M., van Geldern, R., Breisig, S., Buggisch, W. & Day, J. Oxygen isotope evolution of biogenic calcite and apatite during the Middle and Late Devonian. *Int. J. Earth Sci.* **93**, 542–553 (2004).
30. Bassett, D., MacLeod, K., Miller, J. F. & Ethington, R. L. Oxygen isotopic composition of biogenic phosphate and the temperature of Early Ordovician seawater. *Palaios* **22**, 98–103 (2007).
31. Rigo, M. & Joachimski, M. M. Palaeoecology of Late Triassic conodonts: Constraints from oxygen isotopes in biogenic apatite. *Acta Pal. Pol* **55**, 471–478 (2010).
32. Bergmann, K. D. *et al*. A paired apatite and calcite clumped isotope thermometry approach to estimating Cambro-Ordovician seawater temperatures and isotopic composition. *Geochim. Cosmochim. Acta* **224**, 18–41 (2018).
33. Trotter, J. A., Williams, I. S., Barnes, C. R., Männik, P. & Simpson, A. New conodont $\delta^{18}O$ records of Silurian climate change: Implications for environmental and biological events. *Palaeogeogr. Palaeoclimatol. Palaeoecol* **443**, 34–48 (2016).
34. Roelofs, B. *et al*. Assessing the fidelity of marine vertebrate microfossil $\delta^{18}O$ signatures and their potential for palaeo-ecological and –climatic reconstructions. *Palaeogeogr. Palaeoclimatol. Palaeoecol* **465**, 79–92 (2017).
35. Chen, J. *et al*. High-resolution SIMS oxygen isotope analysis on conodont apatite from South China and implications for the end-Permian mass extinction. *Palaeogeogr. Palaeoclimatol. Palaeoecol* **448**, 26–38 (2016).
36. Wheeley, J. R., Smith, M. P. & Boomer, I. Oxygen isotope variability in conodonts: implications for reconstructing Palaeozoic palaeoclimates and palaeooceanography. *J. Geol. Soc.* **169**, 239–250 (2012).
37. Rigo, M., Trotter, J. A., Preto, N. & Williams, I. S. Oxygen isotopic evidence for Late Triassic monsoonal upwelling in the northwestern Tethys. *Geology* **40**, 515–518 (2012).
38. Zhao, Y. *et al*. Proposed Global Standard Stratotype-Section and Point for the base of the Mialongian series and Wuliuan stage (provisional Cambrian Series 3 and Stage 5). Proposal, prepared for the International Subcommission on Cambrian Stratigraphy, 46 pp. (2016).
39. Brasier, M. D. & Sukhov, S. S. The falling amplitude of carbon isotope oscillations through the Lower to Middle Cambrian: Northern Siberia data. *Can. J. Earth Sci.* **35**, 353–373 (1998).
40. Kouchinsky, A. S. *et al*. The SPICE carbon excursion in Siberia: a combined study of the upper Middle Cambrian–lowermost Ordovician Kulyumbe River section, northwestern Siberian Platform. *Geol. Mag.* **145**, 609–622 (2008).
41. Kouchinsky, A., Bengtson, S., Clausen, S. & Vendrasco, M. J. An early Cambrian fauna of skeletal fossils from the Emyaksin Formation, northern Siberia. *Acta Pal. Pol* **60**, 421–512 (2015).
42. Kouchinsky, A. *et al*. A middle Cambrian fauna of skeletal fossils from the Kuonamka Formation, northern Siberia. *Alcheringa* **35**, 123–189 (2011).
43. Gradstein, F. M., Ogg, J. G., Schmitz, M. D. & Ogg, G. M. *The Geologic Time Scale 2012, Volume 2*. Elsevier BV, 1144 pp. (2012).
44. Lécuyer, C., Amiot, R., Touzeau, A. & Trotter, J. Calibration of the phosphate $\delta^{18}O$ thermometer with carbonate-water oxygen fraction equations. *Chem. Geol.* **347**, 217–226 (2013).

45. Lhomme, N. & Clarke, G. K. C. Global budget of water isotopes inferred from polar ice sheets. *Geophys. Res. Lett.* **32**, L20502 (2005).
46. Kolodny, Y., Luz, B., Sander, M. & Clemens, W. A. Dinosaur bones: fossils or pseudomorphs? The pitfalls of physiology reconstruction from apatitic fossils. *Palaeogeogr. Palaeoclimatol. Palaeoecol* **126**, 161–171 (1996).
47. Sharp, Z. D., Atudorei, V. & Furrer, H. The effect of diagenesis on oxygen isotope ratios of biogenic phosphates. *Am. J. Sci* **300**, 222–237 (2000).
48. O'Neil, J. R., Roe, J. L., Reinhardt, E. & Blake, R. E. A rapid and precise method of oxygen isotope analysis of biogenic phosphate. *Isr. J. Earth Sci* **43**, 203–212 (1994).
49. Kocsis, L., Dulai, A., Bitner, M. A., Vennemann, T. & Cooper, M. Geochemical compositions of Neogene phosphatic brachiopods: Implications for ancient environmental and marine conditions. *Palaeogeogr. Palaeoclimatol. Palaeoecol* **326–328**, 66–77 (2012).
50. Rodland, D. L., Kowalewski, M., Dettman, D. L., Flessa, K. W., Atudorei, V. & Sharp, Z. D. High-resolution analysis of δ18O in the biogenic phosphate of modern and fossil lingulid brachiopods. *J. Geol.* **111**, 441–453 (2003).
51. Kolodny, Y., Luz, B. & Navon, O. Oxygen isotope variations in phosphate of biogenic apatites, I. Fish bone apatite – rechecking the rules of the game. *Earth Planet. Sci. Lett.* **64**, 398–404 (1983).
52. Pucéat, E. *et al*. Revised phosphate-water fractionation equation reassessing paleotemperatures derived from biogenic apatite. *Earth Planet. Sci. Lett.* **298**, 135–142 (2010).
53. Sun, Y. *et al*. Chemical and oxygen isotope composition of gem-quality apatites: Implications for oxygen isotope reference materials for secondary ion mass spectrometry (SIMS). *Chem. Geol.* **440**, 164–178 (2016).
54. Žigaitė, Ž. & Whitehouse, M. Stable oxygen isotopes of dental biomineral: differentiation at the intra- and inter-tissue level of modern shark teeth. *GFF* **136**, 337–340 (2014).
55. Brock, G. A. *et al*. Palaeobiogeographic affinities of Australian Cambrian Faunas. *Mem. Ass. Austral. Pal* **23**, 1–61 (2000).
56. Nardin, E. *et al*. Modeling the early Paleozoic long-term climatic trend. *GSA Bull* **123**, 1181–1192 (2011).
57. Sun, Y. *et al*. Lethally hot temperatures during the Early Triassic greenhouse. *Science* **338**, 366–370 (2012).
58. Littler, K., Robinson, S. A., Bown, P. R., Nederbragt, A. J. & Pancost, R. D. High sea-surface temperatures during the Early Cretaceous Epoch. *Nat. Geosci.* **4**, 169–172 (2011).
59. Alsenz, H. *et al*. Sea surface temperature record of a Late Cretaceous tropical Southern Tethys upwelling system. *Palaeogeogr. Palaeoclimatol. Palaeoecol* **392**, 350–358 (2013).
60. World Sea Temperatures, https://www.seatemperature.org/ (12-Feb-2018 & 15-Aug-2018).
61. Brock, T. D. Life at high temperatures. *Science* **230**, 132–138 (1985).
62. Compton, T. J., Rijkenverg, M. J. A., Drent, J. & Piersma, T. Thermal tolerance ranges and climate variability: A comparison between bivalves from differing climates. *J. Exp. Mar. Biol. Ecol.* **352**, 200–211 (2007).
63. Rothschild, L. J. & Mancinelli, R. L. Life in extreme environments. *Nature* **409**, 1092–1101 (2001).
64. Kinne, O. Marine Ecology: A Comprehensive, Integrated Treatise on Life in Oceans and Coastal Waters. Volume I: Environmental Factors, Part 1. Wiley-Interscience, 681 pp. (1970).
65. Kita, N. T., Ushikubo, T., Fu, B. & Valley, J. W. High precision SIMS oxygen isotope analysis and the effect of sample topography. *Chem. Geol.* **264**, 43–57 (2009).
66. Whitehouse, M. J. & Nemchin, A. N. High precision, high accuracy measurement of oxygen isotopes in a large lunar zircon by SIMS. *Chem. Geol.* **261**, 32–42 (2009).

Acknowledgements

We acknowledge financial support from SYNTHESYS (SE-TAF 6454 to T.W.) which was financed by the European Community – Research Infrastructure Action under the Seventh Framework Program. We thank K. Lindén and L. Ilyinsky for sample preparation prior to ion microprobe analyses. SEM and EDS analyses were aided by H. Cieszynski and S. Gilbricht.

Author Contributions

T.W. conceived the study. A.K. collected samples used in this study. T.W., M.W. and C.B.S. did the analyses. T.W. wrote the manuscript, with contributions from C.B.S., M.W. and A.K. All authors contributed to the discussions and interpretations of the data.

Additional Information

Supplementary information accompanies this paper at https://doi.org/10.1038/s41598-019-42719-4.

Competing Interests: The authors declare no competing interests.

Publisher's note: Springer Nature remains neutral with regard to jurisdictional claims in published maps and institutional affiliations.